Optical frequency comb generation by pulsed pumping

Marcin Malinowski,[1] Ashutosh Rao,[1] Peter Delfyett,[1,2] and Sasan Fathpour[1,2]

[1)] *CREOL, The College of Optics and Photonics, University of Central Florida, Orlando, Florida 32816, USA*

[2)] *Department of Electrical and Computer Engineering, University of Central Florida, Orlando, Florida 32816, USA*

(Dated: 24 April 2017)

A synchronously-pumped Kerr cavity is proposed and studied for power-efficient frequency comb generation in optical microring resonators. The system is modeled using the Lugiato-Lefever equation. Analytical solutions are provided for an ideal case, and extended by numerical methods to account for optical loss and higher orders of dispersion. It is shown that the average power requirement is reduced by the duty cycle of the pulse with respect to conventional continuous-wave-pumped microrings and it is significantly lower than pulsed pumping of straight waveguides.

Frequency combs are composed of a series of short and high-power pulses in the time domain that translate into a broad comb in the frequency domain. This duality translates into a host of applications for optical combs[1,2]. For instance, the broad spectrum facilitates spectroscopy in regimes from the ultraviolet (UV) to the infrared (IR)[3], wherein high peak power of the pulses is necessary for precision distance measurements to overcome noise[4]. Atomic clocks, where combs are used to count the optical cycles, is another important application[5]. In conjunction with the quest for miniaturization, there has been a strive towards reducing the footprint of frequency optical comb sources using continuous-wave (CW) pump sources. The first step was the demonstration of frequency comb generation in whispering-gallery mode resonators[6,7], followed by a demonstration of on-chip frequency comb generation on silicon nitride[8]. The transition from smooth laser-ablated structures to etched waveguides, however, came at the expense of higher threshold power (e.g. ≈ 1.3 W)[8]. Additionally, the conversion efficiency for generation of frequency combs is low and on the order of 1 to 2% for CW pumping[9].

To overcome this power-efficiency shortcoming, we have previously proposed pulsed pumping in a fully integrated on-chip frequency comb source[10]. The notion of a synchronously-pumped Kerr cavity was first theoretically explored in fibers[11]. The system has drawn particular interest due to its chaotic and bistable behavior[12]. Synchronous pumping with sinusoidal input, coming from a beat signal of two CW sources, was first suggested in[13] as a means of frequency comb generation. Furthermore, wide Gaussian pulses with sinusoidal modulation are proposed for storing solitons in optical memory devices[14]. A synchronously-pumped fiber Kerr cavity has been studied in optical fibers for observing spontaneous symmetry breaking[15]. Soliton formation in a 10 GHz fiber cavity pumped by picosecond pulses has recently been demonstrated experimentally[16].

In this letter, synchronous pulsed pumping is studied for the first time in the context of octave-spanning optical comb generation in integrated microring resonators. Microrings offer the possibility of a compact, chip-size stable frequency comb source. The Lugiato-Lefever model is employed here[17], which can be shown to be equivalent to the coupled-mode equations formalism[17]. We show that for broadband frequency comb generation, essential for f-2f referencing, the large dispersion slope, (β_3), of the microring resonators results in generation of Cherenkov radiation and a change in the solitons group velocity that has to be compensated by adjusting the repetition rate of the driving pulse train. Such an effect is not

observed in the aforementioned narrow-band synchronously-pumped fiber-based combs[16], due to lower dispersion in fibers. The power efficiency of the proposed approach is explored and design and modeling guidelines are developed.

The paper is structured as follows. We first present an analytical expression for a special lossless case with a soliton pulse pump, sech(τ), to develop basic understanding of the system behavior. Next, losses are included for a sweep of Gaussian input pulses where the pulse width is varied. Next, we add a third order dispersion term and discuss the effects of Cherenkov radiation. Finally, an experimentally feasible 10-GHz ring architecture pumped by a mode-locked laser is simulated and compared against both CW pumping of microrings, as well as pulsed pumping of straight waveguides.

The Lugiato-Lefever (LL) equation[17] is a mean-field model of microresonator behavior, where the effect of coupling is averaged over each roundtrip. The two equations from Ikeda map approach governing pulse propagation and periodic boundary conditions are reduced to one making it computationally more efficient[18]. The full LL equation is

$$t_r \frac{\partial A}{\partial t} = [-\frac{\alpha+\theta}{2} - i\delta_0 + iL\sum_{k>2}\frac{\beta_k}{k!}(i\frac{\partial}{\partial\tau})^k + iL\eta|A|^2]A + \sqrt{\theta}A_{in}, \tag{1}$$

where t is the slow time of the cavity (duration of multiple roundtrips), τ is the fast time in the moving frame of reference, α is the integrated loss, θ is the coupling loss, L is the length of the cavity, t_r is the round trip time, δ_0 is the detuning or the phase difference between driving field and the cavity resonance, η is the Kerr non-linearity coefficient ($= \frac{2\pi n_2}{\lambda_p A_{eff}}$), where A_{in} is the envelope of the pump field and A is the envelope of the field in the cavity.

In the next section, only the second-order anomalous dispersion (β_2) is retained and the normalized version of the same equation is used[19], i.e.,

$$\frac{\partial A}{\partial t} = [-1 - i\Delta + i\frac{\partial^2}{\partial\tau^2} + i|A|^2]A + A_{in}(\tau). \tag{2}$$

The normalization is achieved via the following transformations: $t \to (\theta+\alpha)t/2t_r$, $A \to \sqrt{2L\eta/(\alpha+\theta)}A$, $\tau \to \sqrt{(\alpha+\theta)/L|\beta_2|}\tau$, $\Delta = 2\delta_0/(\alpha+\theta)$ and $A_{in} \to \sqrt{8L\theta\eta/(\alpha+\theta)^3}A_{in}$.

First, we note that there exists an analytical solution to the steady state[13], lossless LL equation

$$[-i\Delta + i\frac{\partial^2}{\partial\tau^2} + i|A|^2]A + A_{in}(\tau) = 0, \tag{3}$$

when the input and the field inside the cavity are given by

$$A_{in}(\tau) = \frac{C_1}{\cosh(C_2\tau)}, \qquad A(\tau) = \frac{C_3}{\cosh(C_2\tau)}, \tag{4}$$

with the coefficients related by $|C_3| = \sqrt{2}C_2$ and $\Delta C_3 - 1/2|C_3|^2 C_3 + iC_1 = 0$. Physical intuition suggests that if the input pulse is wide, it can be locally approximated as a constant background for which the stable solutions are known. Mathematically, this concept is encompassed by the method of matched asymptotics. For $\tau << 1$, A_{in} is constant, i.e., $A_{in} = C_1$, and the stable solution to (3) is known[20]. Far away from the center of the pulse $\tau = 0$, the solution is just the soliton obtained from (4). The field inside the cavity is the sum of these two minus the overlap at $\tau = \infty$. Following this prescription, the compressed pulse is given by

$$A(\tau) = \frac{C_3}{\cosh(C_2\tau)} + \frac{2A_0 \sinh^2\alpha}{1 - \cosh\alpha\cosh(B\tau)}, \tag{5}$$

where the coefficients are related implicitly via α as

$$C_1 = i\frac{\sqrt{4\Delta^3}\cosh^2\alpha}{(1+2\cosh^2\alpha)^{3/2}} \qquad A_0 = \sqrt{\Delta/(1+2\cosh^2\alpha)}, \tag{6}$$

and $B = \sqrt{2}A_0 \sinh\alpha$.

The relation for coefficients of eq. (4) is a third-order polynomial, thus in principle there can be three solutions of C_3, the smallest of which (widest pulses) was found to be stable. Also, two solutions are available for a constant pump power (CW) case, referred to as ψ_+ and ψ_- in[20]. ψ_- is stable and has been used in the construction of the solutions presented in (5). Excellent agreement between the above approximate analytical solution and the numerical solutions, produced by the Newton-Raphson method, is evident in Fig. 1.

Since the output solitons formed from pulses have the same shape as those formed from a CW pump, it can be inferred that when the locally flat approximation holds for input pulses, the average power requirement for a pulse pump will be a fraction of the CW power, that is the duty cycle of the pulse with respect to CW. This is an important, yet simple, finding of this work for comb generation in microring structures.

So far for the analytical treatment, loss was not considered in eq. (2). In the next section we retain it and use Gaussian pulses, $\exp(-\tau/\tau_p)^2$, for the input field. A computationally efficient method of investigating the steady state solutions utilizes a Newton-Raphson (NR)

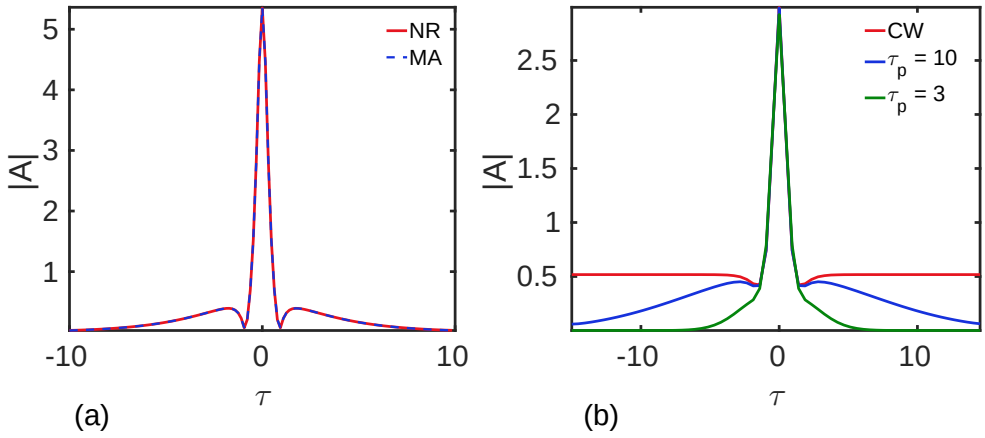

FIG. 1: (a) Excellent agreement between the matched asymptotics (MA) method and the numerical solution from the Newton-Raphson (NR) solver plotted for $\Delta = 12$, zero loss and $C_1 = 6$. (b) Solitons formed from Gaussian pulses, $\exp -(\tau/\tau_p)^2$, are the same as those from CW background provided that the loss and the detuning is the same ($\Delta = 4$), and the peak power of the pulse is equal to the CW background ($A_{in} = 2$). All solutions are stable, as confirmed using the split-step Fourier time evolution method.

solver[21] and a continuation method[20]. The single soliton state for the CW case, generated by the split-step Fourier method time-evolution code[22], is used as the initial guess for a NR solver. We wish to find a steady-state solution to the case of pulse pumping while knowing the solution to the CW case. Thus, we use a NR solver to smoothly transform the solution from the extreme case $\tau_p = \infty$ i.e. CW case to that of the desired input pulse width. The peak power and the detuning has to remain constant in this transformation. The steady state solutions are plotted in Fig. 1. The stability of the solutions is confirmed by time-evolving them in the split-step Fourier method code with initial amplitude noise (max amplitude 10^{-7}). The noise is added to seed any potential instabilities. It is evident that the solitons formed from pulses have the same functional form as those formed from the CW case. The observation remains valid for relatively short pulses $\tau_p = 3$ in comparison to solitons with a full-width at half maximun (FWHM) of 1.25 and for different pump powers and detunings, as long as the undesired spontaneous symmetry breaking does not occur. The temporal symmetry breaking manifests itself as the soliton forming on one side of the input pulse[15].

We also confirmed that soliton formation (pulse compression) can be achieved starting

from Gaussian pulses themselves. The time evolution of the LL equation is studied using the split-step Fourier method. The detuning is changed non-adiabatically to induce various phases. First, as in the CW case[22], the modulation instability develops on top of the input pulses. Next after and abrupt increase of detuning, unstable breathing solitons appear that coalesce and break apart. Finally, the detning is adjusted to obtain a stable single soliton phase. An example of such evolution is shown in Fig. 2a. The compression can be also achieved via increasing the input pulse power in abrupt steps.

Next, we add a third order dispersion term. To accentuate the effects the term is arbitrarily chosen as $-0.12\frac{\partial^3 A}{\partial \tau^3}$. The additional dispersion term perturbs the solitons and results in an emission of a dispersive wave, referred to as Cherenkov radiation[21,23]. The dispersive wave creates an additional peak in the spectrum, but more importantly leads to a temporal drift of solitons in the moving reference frame. Since the drift velocity is constant, this would experimentally correspond to a change of the spacing of comb lines. It also means that, in the simulations, the pump pulse has to drift with the solitons to form stable solutions, as demonstrated in Fig.2b. If the pump is allowed to drift with the solitons, all the above-discussed observations regarding soliton formation remain valid.

Finally, realistic simulations on a specific material system for a microring cavity are presented here utilizing the full Lugiato-Lefever equation (1). The physical parameters are borrowed from our recent experimental results on chalcogenide glass ($Ge_{23}Sb_7S_{70}$)[24], as well as further dispersion and nonlinear index measurements we have performed on the material. The platform's loss has been steadily decreasing[24,25]. Accordingly, the following values are assumed: 2 mm radius corresponding to 10 GHz FSR, $\gamma = 1.92$ W^{-1} m^{-1}, propagation loss of 0.2 dB/cm, critical coupling, and $\beta_2 = -6.9 \times 10^{-26}$ s^2 m^{-1}. It is noted that chalcogenide glasses have higher nonlinear coefficient than silicon nitride which has been used for frequency comb generation[8]. The higher nonlinearity of the material can compensate for the higher losses, as verified by our models. Supercontinuum generation on this platform has been demonstrated experimentally by our collaborators and us[26].

Regardless of the material system choice, the power requirement is reduced by the duty cycle of the pulse with respect to the CW case. The simulated field inside the cavity and the corresponding spectra are shown in Fig. 3. For an octave spanning spectrum generated in a 10 GHz system, the CW power requirement in the bus waveguide was found to be 10 W, which is experimentally hard to achieve. It is reduced to a manageable average power of

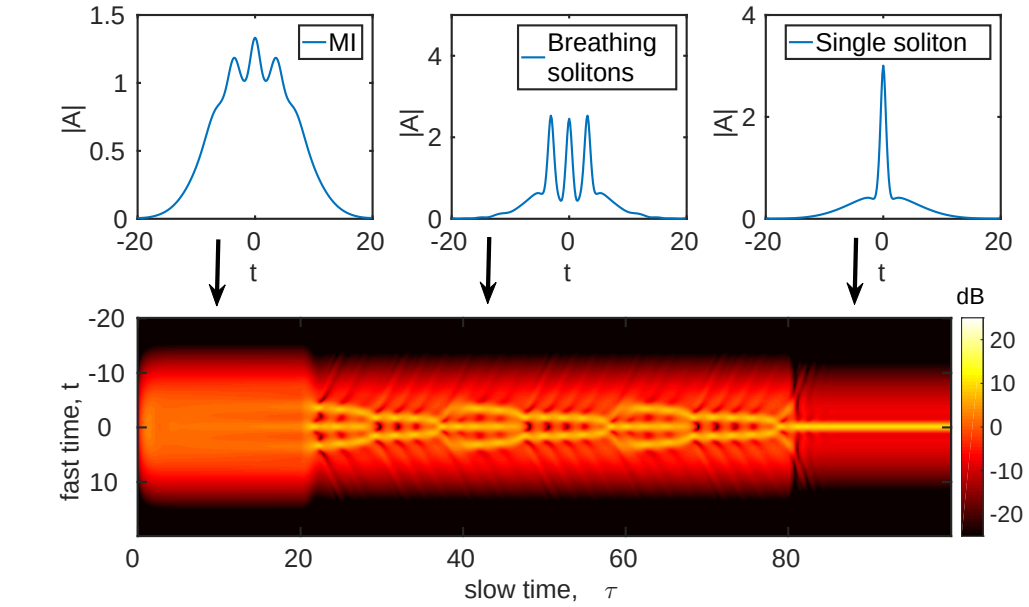

(a)

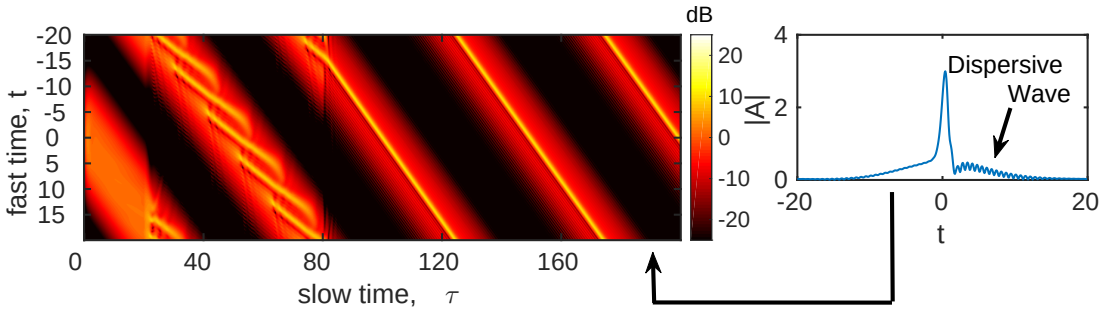

(b)

FIG. 2: (a) The path towards pulse compression (single soliton formation) closely follows that of the CW case. The plot shows the power in the cavity on a log scale and corresponding selected snapshots. Initially the pulses develop modulational instability (MI) for $\Delta = 0, t < 20$. After an abrupt increase in the detuning at $t = 20, \Delta = 2$, unstable breathing solitons appear that coalesce and break apart, at $\Delta = 4.16, t = 80$ they condense on a stable single soliton solution. Simulation performed for Gaussian input pulse, $2.0\exp(-(\tau/10)^2)$. (b) The same simulation parameters as in (a) are used except that 3rd order dispersion is added, $-0.12\frac{\partial^3 A}{\partial \tau^3}$, this causes the soliton to emit a dispersive wave (Cherenkov radiation) that affects it's group velocity, the soliton drifts in the simulation in the moving frame of reference. For the single soliton state to be stable the input pulse has to also drift (the repetition of the input pulses has to be adjusted).

130 mW (1.3%) for Gaussian input pulses ($\tau_p = 1$ ps), and 200 mW (2%) for more realistic breathing mode-locked lasers that could be integrated on the same chip[27,28].

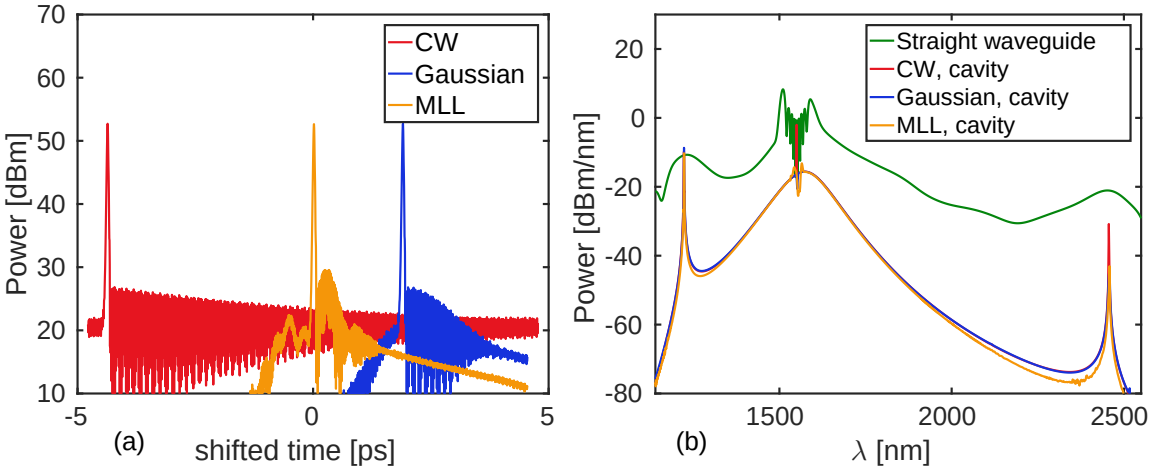

FIG. 3: (a) Comparison of compressed pulses in the 100 ps ring cavity plotted together inside a 10 ps window. The Gaussian in all plots corresponds to width of $\tau_p = 1$ ps and MLL is a breathing mode-locked laser. The solitons formed inside the ring cavity are the same provided that the peak of the pulse is the same as the CW background. The oscillations present next to the solitons is the Chernekov radiation. (b) Octave spanning spectra of the pulses from (a) after coupling into the bus waveguide. Also shown is the case of supercontinuum generation in straight waveguides using Gaussian input pulses. For the supercontinuum to reach similar bandwidth as in the case of a cavity, the average power has to be 8 time higher.

It is known that pulse compression can be also achieved in straight waveguides[29], thus a comparison of the power efficiency with this approach would be useful. As summarized in Fig. 3, for Gaussian pulses with $\tau_p = 1$ ps, the required peak power is 80 W in order to attain similar comb bandwidths of the microring cases. This power is 8 times higher than the above synchronously-pumped microring cavity. The optimal propagation distance for which the spectrum is the broadest was found to be 30 cm, which demonstrates that, on top of better power efficiency, the rings provide compactness for the same performance but at the expense of increased complexity in the system architecture, as discussed above. The spectrum of the supercontinuum from straight waveguides is flatter, but the waveguide dispersion was designed such that Cherenkov radiation boosts the power of the microring spectra at the short (1223 nm) and long (2456 nm) side. This is essential for f-2f referencing.

Pulsed pumping of a microring cavity is more complicated than using CW pump, nevertheless we believe that it is experimentally feasible. Such a system has been demonstrated in fiber cavities[23] and it could be transferred to microring resonators, as outlined in the following. For precise control of the cavity detuning, part of the MLL beam could be tapped off and injected into the laser in the counterpropagating direction. Locking would be achieved by monitoring the coupled power. The low power of the counterpropagating beam would ensure locking of the carrier frequency to the closest CW resonance, thus detuning of the main beam could be precisely controlled using for example a phase modulator. Consequently, the soliton formation process of Fig. 2a would be experimentally possible. Either the MLL or the cavity could be controlled thermally to achieve matching of the FSRs. Furthermore, Ref.[16] demonstrates that for a 10-GHz fiber cavity, the soliton remains locked to the driving pulse train over 10s of kHz, thus exact FSR matching may not be necessary. The important finding of the present work is that in microrings, which are much more dispersive than fibers, the soliton emits a dispersive wave that results in solitons with different group velocity than the CW light case. This difference in FSRs of the soliton and the cold cavity is constant and can be extracted from the simulations and will have to be taken into account in the actual experiment. Finally, we note that using a MLL is conceptually similar to using a CW light modulated at the repetition rate of the cavity[30], which supports the feasibility of the proposed scheme. Also, Ref.[30] has shown that parametric seeding has an added benefit of suppressing undesirable non-equidistant combs.

In conclusion, synchronously-pumped Kerr cavity is proposed for octave spanning frequency comb generation in integrated microrings and its power efficiency benefits are analytically and numerically modeled. It is demonstrated that for pulsed input, solitons remain the fundamental solution of the system, and hence the power requirement is reduced by the duty cycle of the pulse with respect to CW pumping of the same rings. When compared with straight waveguides, the proposed approach benefits from the power enhancement of the microring and hence again lower power requirement.

This research was developed with funding from the Defense Advanced Research Projects Agency (DARPA). The views, opinions and/or findings expressed are those of the authors and should not be interpreted as representing the official views or policies of the Department of Defense or the U.S. Government. We also thank Meer Nazmus Sakib for performing chalcogenide depositions, Seyfollah Toroghi for dispersion measurement and Akbar Ali Syed

for z-scan measurements of n_2.

REFERENCES

[1]T. J. Kippenberg, R. Holzwarth, and S. A. Diddams, "Microresonator-based optical frequency combs," Science **332**, 555–559 (2011).

[2]P. Delfyett, I. Ozdur, N. Hoghooghi, M. Akbulut, J. Davila-Rodriguez, and S. Bhooplapur, "Advanced ultrafast technologies based on optical frequency combs," Selected Topics in Quantum Electronics, IEEE Journal of **18**, 258–274 (2012).

[3]F. Keilmann, C. Gohle, and R. Holzwarth, "Time-domain mid-infrared frequency-comb spectrometer," Opt. Lett. **29**, 1542–1544 (2004).

[4]I. Coddington, W. Swann, L. Nenadovic, and N. Newbury, "Rapid and precise absolute distance measurements at long range," Nature Photonics **3**, 351–356 (2009).

[5]S. A. Diddams, T. Udem, J. C. Bergquist, E. A. Curtis, R. E. Drullinger, L. Hollberg, W. M. Itano, W. D. Lee, C. W. Oates, K. R. Vogel, and D. J. Wineland, "An optical clock based on a single trapped 199 Hg+ ion," Science **293**, 825–828 (2001).

[6]P. DelHaye, A. Schliesser, O. Arcizet, T. Wilken, R. Holzwarth, and T. Kippenberg, "Optical frequency comb generation from a monolithic microresonator," Nature **450**, 1214–1217 (2007).

[7]I. S. Grudinin, N. Yu, and L. Maleki, "Generation of optical frequency combs with a CaF2 resonator," Opt. Lett. **34**, 878–880 (2009).

[8]Y. Okawachi, K. Saha, J. S. Levy, Y. H. Wen, M. Lipson, and A. L. Gaeta, "Octave-spanning frequency comb generation in a silicon nitride chip," Opt. Lett. **36**, 3398–3400 (2011).

[9]C. Bao, L. Zhang, A. Matsko, Y. Yan, Z. Zhao, G. Xie, A. M. Agarwal, L. C. Kimerling, J. Michel, L. Maleki, and A. E. Willner, "Nonlinear conversion efficiency in Kerr frequency comb generation," Opt. Lett. **39**, 6126–6129 (2014).

[10]M. Malinowski, A. Rao, P. Delfyett, and S. Fathpour, "Synchronously-pumped microring resonator for efficient optical comb generation," in *Conference on Lasers and Electro-Optics* (Optical Society of America, 2016) p. JTu5A.50.

[11]J. Garca-Mateos, F. C. Bienzobas, and M. Haelterman, "Optical bistability and temporal symmetry-breaking instability in nonlinear fiber resonators," Fiber and Integrated Optics

14, 337–346 (1995).

[12]K. J. Blow and N. J. Doran, "Global and local chaos in the pumped nonlinear Schrödinger equation," Phys. Rev. Lett. **52**, 526–529 (1984).

[13]M. Haelterman, S. Trillo, and S. Wabnitz, "Generation of ultrahigh repetition rate soliton trains in fibre ring," Electronics Letters **29**, 119– (1993).

[14]G. S. McDonald and W. J. Firth, "Spatial solitary-wave optical memory," J. Opt. Soc. Am. B **7**, 1328–1335 (1990).

[15]Y. Xu and S. Coen, "Experimental observation of the spontaneous breaking of the time-reversal symmetry in a synchronously pumped passive Kerr resonator," Opt. Lett. **39**, 3492–3495 (2014).

[16]E. Obrzud, S. Lecomte, and T. Herr, "Temporal solitons in microresonators driven by optical pulses," arXiv preprint arXiv:1612.08993 (2016).

[17]L. A. Lugiato and R. Lefever, "Spatial dissipative structures in passive optical systems," Phys. Rev. Lett. **58**, 2209–2211 (1987).

[18]M. J. Schmidberger, D. Novoa, F. Biancalana, P. S. Russell, and N. Y. Joly, "Multistability and spontaneous breaking in pulse-shape symmetry in fiber ring cavities," Opt. Express **22**, 3045–3053 (2014).

[19]S. Coen and M. Erkintalo, "Universal scaling laws of Kerr frequency combs," Opt. Lett. **38**, 1790–1792 (2013).

[20]I. V. Barashenkov and Y. S. Smirnov, "Existence and stability chart for the ac-driven, damped nonlinear Schrödinger solitons," Phys. Rev. E **54**, 5707–5725 (1996).

[21]S. Coen, H. G. Randle, T. Sylvestre, and M. Erkintalo, "Modeling of octave-spanning Kerr frequency combs using a generalized mean-field Lugiato-Lefever model," Opt. Lett. **38**, 37–39 (2013).

[22]M. R. E. Lamont, Y. Okawachi, and A. L. Gaeta, "Route to stabilized ultrabroadband microresonator-based frequency combs," Opt. Lett. **38**, 3478–3481 (2013).

[23]K. Luo, Y. Xu, M. Erkintalo, and S. G. Murdoch, "Resonant radiation in synchronously pumped passive Kerr cavities," Opt. Lett. **40**, 427–430 (2015).

[24]J. Chiles, M. Malinowski, A. Rao, S. Novak, K. Richardson, and S. Fathpour, "Low-loss, submicron chalcogenide integrated photonics with chlorine plasma etching," Applied Physics Letters **106**, 111110 (2015).

[25]Q. Du, Y. Huang, J. Li, D. Kita, J. Michon, H. Lin, L. Li, S. Novak, K. Richardson,

W. Zhang, and J. Hu, "Low-loss photonic device in Ge–Sb–S chalcogenide glass," Opt. Lett. **41**, 3090–3093 (2016).

[26]J. E. Tremblay, Y. H. Lin, M. N. Sakib, M. Malinowski, S. Novak, P. Qiao, C. Chang-Hasnain, K. Richardson, S. Fathpour, and M. C. Wu, "High-q and low-loss chalcogenide waveguide for nonlinear supercontinuum generation," in *2016 IEEE Photonics Conference (IPC)* (2016) pp. 158–159.

[27]B. Resan and P. J. Delfyett, "Dispersion-managed breathing-mode semiconductor mode-locked ring laser: experimental characterization and numerical simulations," Quantum Electronics, IEEE Journal of **40**, 214–221 (2004).

[28]B. Resan, L. Archundia, and P. J. Delfyett, "FROG measured high-power 185-fs pulses generated by down-chirping of the dispersion-managed breathing-mode semiconductor mode-locked laser," Photonics Technology Letters, IEEE **17**, 1384–1386 (2005).

[29]R. Halir, Y. Okawachi, J. S. Levy, M. A. Foster, M. Lipson, and A. L. Gaeta, "Ultra-broadband supercontinuum generation in a CMOS-compatible platform," Opt. Lett. **37**, 1685–1687 (2012).

[30]S. B. Papp, K. Beha, P. DelHaye, F. Quinlan, H. Lee, K. J. Vahala, and S. A. Diddams, "Microresonator frequency comb optical clock," Optica **1**, 10–14 (2014).

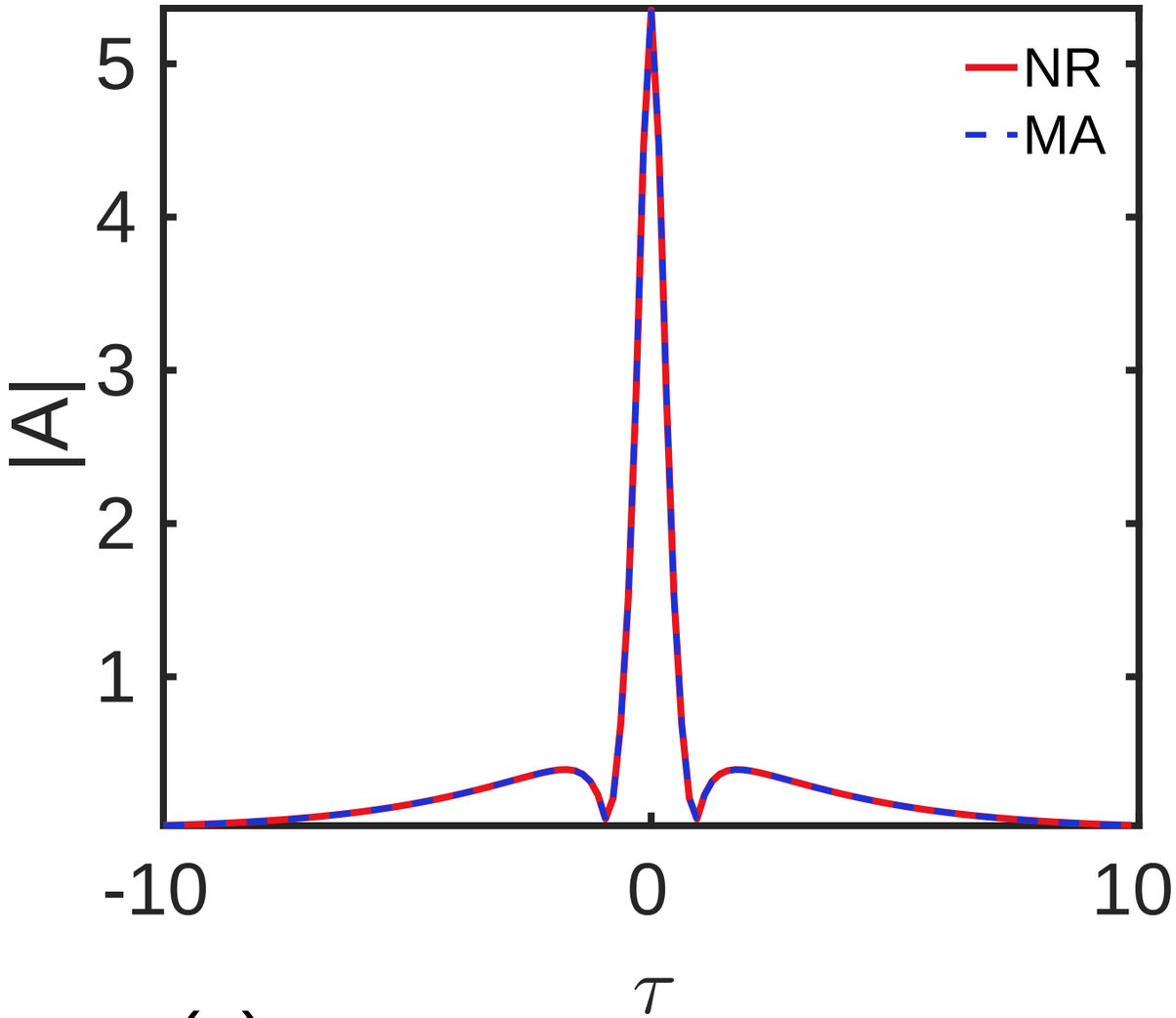

(a)

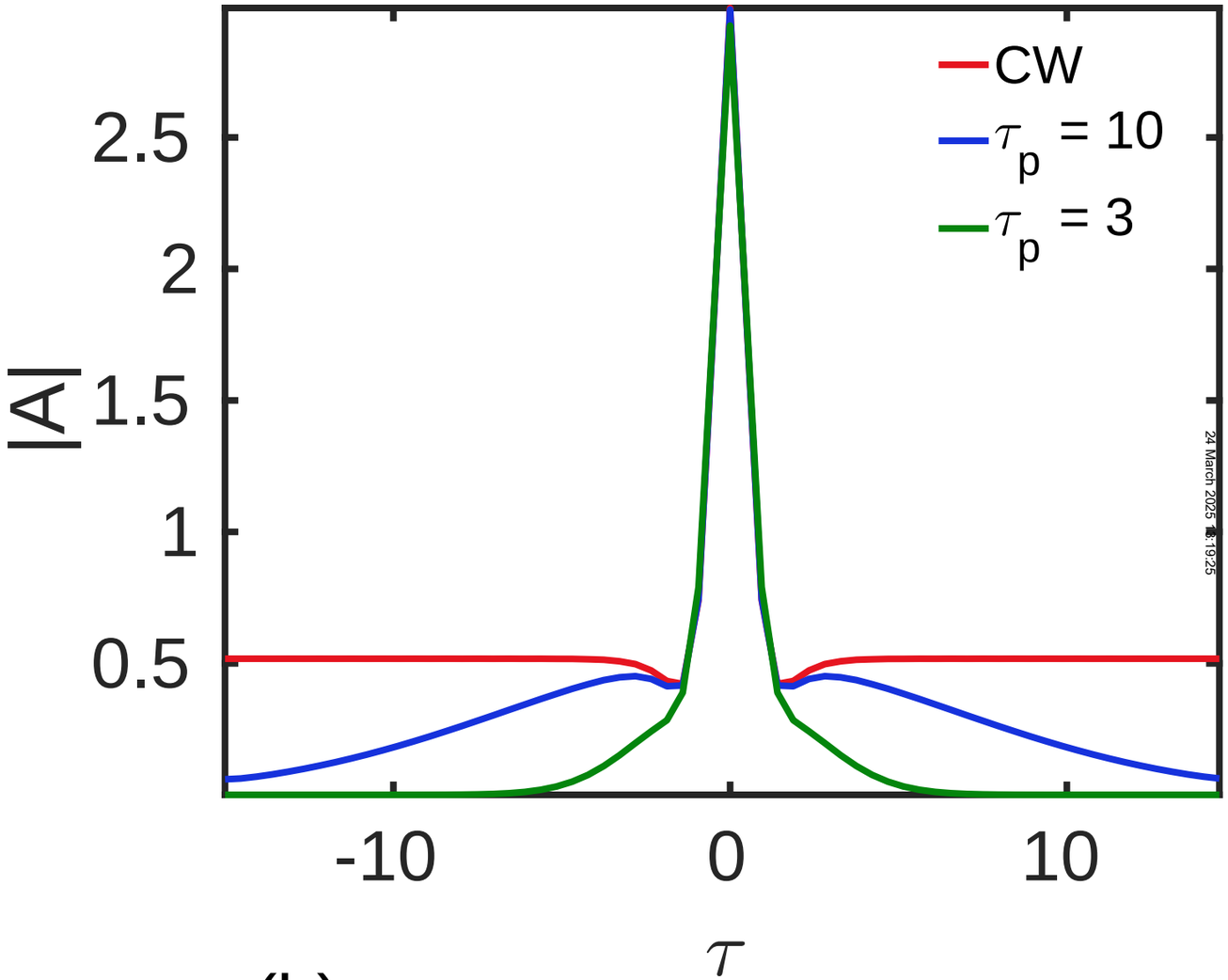

(b)

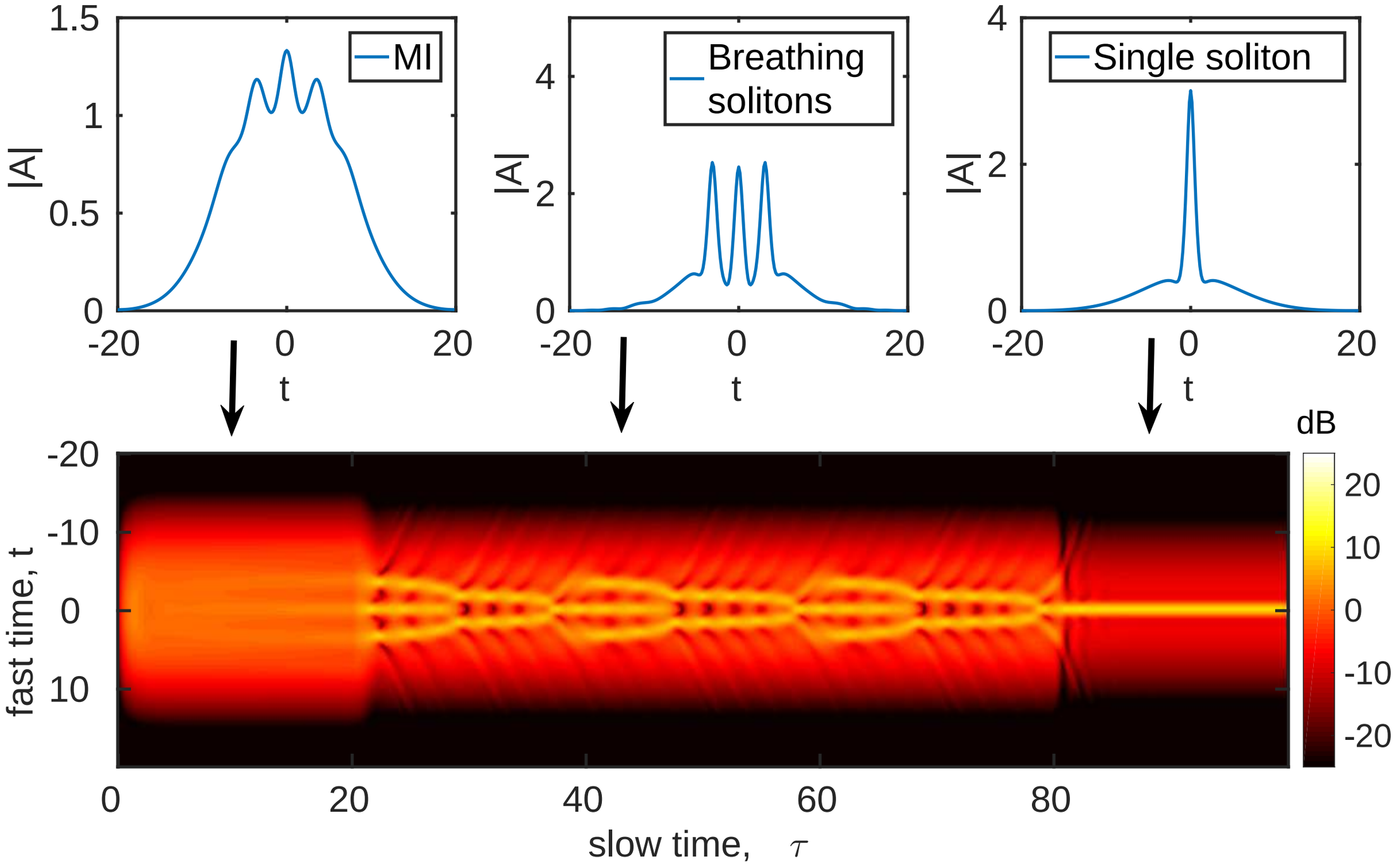

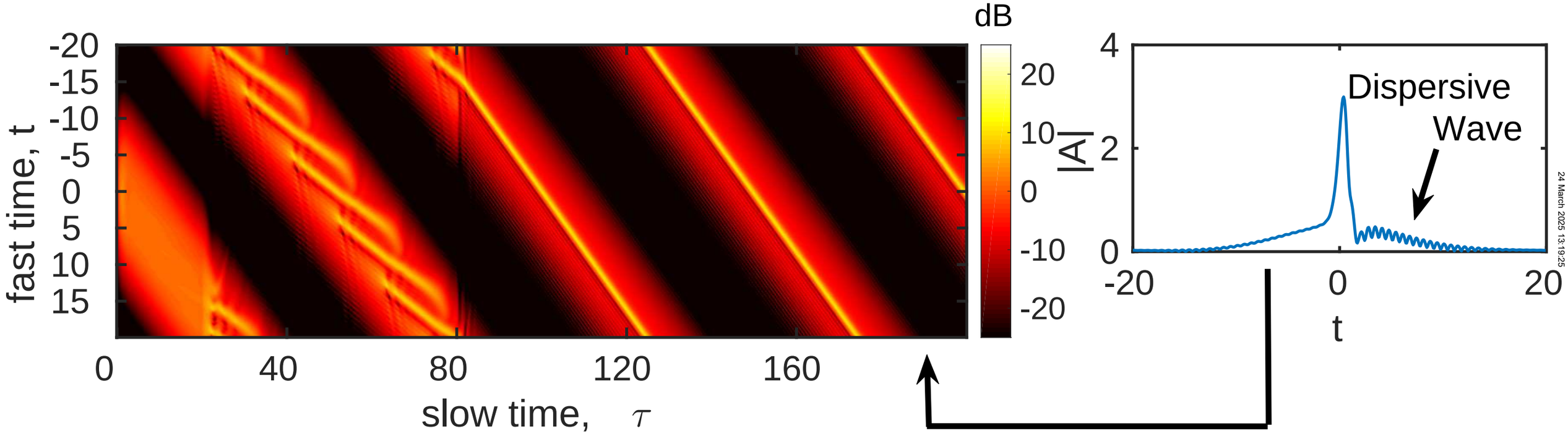
dB
20
10
0
-10
-20
fast time, t
-20
-15
-10
-5
0
5
10
15
0
40
80
120
160
slow time, τ
|A|
4
2
0
-20
0
20
t
Dispersive
Wave
24 March 2025 13:19:25

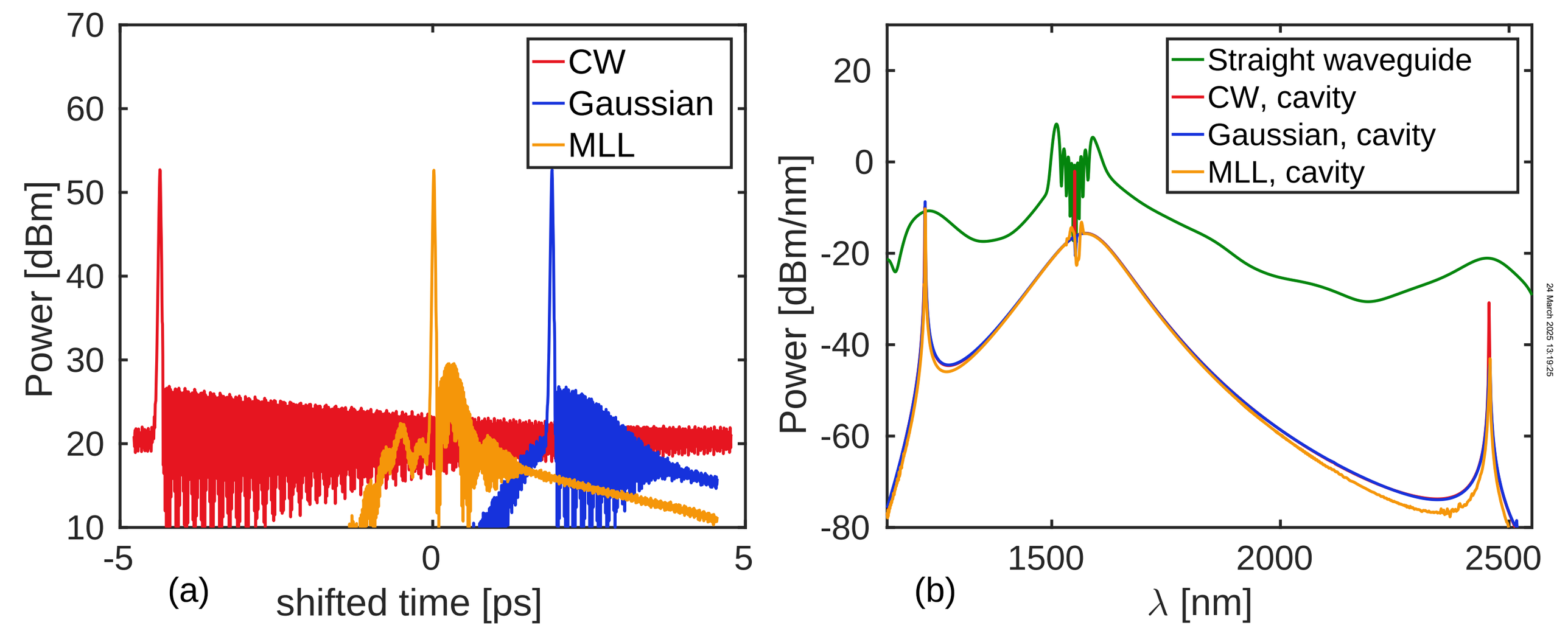
70
60
50
40
30
20
10
Power [dBm]
-5
0
5
shifted time [ps]
(a)
CW
Gaussian
MLL
20
0
-20
-40
-60
-80
Power [dBm/nm]
1500
2000
2500
λ [nm]
(b)
Straight waveguide
CW, cavity
Gaussian, cavity
MLL, cavity
24 March 2025 13:19:25